

Article

# Comparison of Detrital Zircon U-Pb and Muscovite $^{40}\text{Ar}/^{39}\text{Ar}$ Ages in the Yangtze Sediment: Implications for Provenance Studies

Xilin Sun <sup>1,2,\*</sup> , Klaudia F. Kuiper <sup>2</sup>, Yuntao Tian <sup>1</sup>, Chang'an Li <sup>3</sup>, Zengjie Zhang <sup>1</sup> and Jan R. Wijbrans <sup>2</sup> 

<sup>1</sup> School of Earth Sciences and Engineering, Sun Yat-sen University, Guangzhou 510275, China; tianyuntao@mail.sysu.edu.cn (Y.T.); zhangzj55@mail.sysu.edu.cn (Z.Z.)

<sup>2</sup> Department of Earth Sciences, Cluster Geology and Geochemistry, Vrije Universiteit Amsterdam, De Boelelaan 1085, 1081 HV Amsterdam, the Netherlands; k.f.kuiper@vu.nl (K.F.K.); j.r.wijbrans@vu.nl (J.R.W.)

<sup>3</sup> School of Geography and Information Engineering, China University of Geosciences, Wuhan 430074, China; chanli@cug.edu.cn

\* Correspondence: sunxi-lin@163.com

Received: 30 June 2020; Accepted: 17 July 2020; Published: 20 July 2020



**Abstract:** Detrital zircon U-Pb and muscovite  $^{40}\text{Ar}/^{39}\text{Ar}$  dating are useful tools for investigating sediment provenance and regional tectonic histories. However, the two types of data from same sample do not necessarily give consistent results. Here, we compare published detrital muscovite  $^{40}\text{Ar}/^{39}\text{Ar}$  and zircon U-Pb ages of modern sands from the Yangtze River to reveal potential factors controlling differences in their provenance age signals. Detrital muscovite  $^{40}\text{Ar}/^{39}\text{Ar}$  ages of the Major tributaries and Main trunk suggest that the Dadu River is a dominant sediment contributor to the lower Yangtze. However, detrital zircon data suggest that the Yalong, Dadu, and Min rivers are the most important sediment suppliers. This difference could be caused by combined effects of lower reaches dilution, laser spot location on zircons and difference in closure temperature and durability between muscovite and zircon. The bias caused by sediment laser spot targeting a core or rim of zircon and zircon reworking should be considered in provenance studies.

**Keywords:** zircon U-Pb ages; muscovite  $^{40}\text{Ar}/^{39}\text{Ar}$  ages; sediment provenance; Yangtze River

## 1. Introduction

Detrital zircon U-Pb dating is a much used sediment provenance tool, which is commonly used to constrain Maximum sediment depositional ages [1–4], erosion patterns of a river system [5–7], and orogen development of the catchment area [7–9]. Zircon is formed in Magmatic (plutonic or volcanic) or high-temperature metamorphic rocks. The zircon U-Pb ages are generally crystallization or high-grade metamorphism ages, but age signals can be complicated by multiple age zoning [7,10,11]. Muscovite  $^{40}\text{Ar}/^{39}\text{Ar}$  dating is also widely used for isotope provenance studies and is attractive because muscovite provenance data more-readily can be linked to the more recent processes in the hinterland due to its lower closure temperature and lower resistance to weathering. Muscovite is typically derived from low–medium-grade metamorphic rocks or S-type granites and commonly is present in muddy and sandy sediments. Muscovite  $^{40}\text{Ar}/^{39}\text{Ar}$  ages are cooling ages that record cooling of muscovite grains below the closure temperature (350–425 °C [12]). Because zircon's high closure temperature (>900 °C [13]) and resistance to physical and chemical weathering, it can survive multiple cycles of metamorphic overprinting, weathering, erosion and deposition. In contrast, muscovite is less likely to survive multiple orogenic events because of isotopic resetting or destruction. Detrital zircon ages

record old Magmatic or high-grade metamorphic events of source area and often fail to record the most recent metamorphic or Magmatic event [10,14,15]. Detrital muscovite  $^{40}\text{Ar}/^{39}\text{Ar}$  age distributions are commonly simpler and contain the records of the more-recent parts of the tectonic history of a source area. Detrital zircon and muscovite ages of the same sample always give significantly different age distributions and therefore complicate interpretations of sediment provenance [10,16]. The possible factors (difference in closure temperature and durability) have been assessed in previous studies [10,16], but do not fully explain observed differences in sediment provenance based on either of these methods.

The Yangtze River, as the longest river in Asia (Figure 1), is a suitable candidate for assessing factors that control the differences in sediment provenance age signals between zircon and muscovite. Its sediment provenances have been studied intensively by numerous methods, including zircon U-Pb, monazite U-Th-Pb, Pb isotopes of K-feldspar, Nd isotopes, clay mineral composition, and heavy minerals composition [17–24]. Further, previous studies have also reported a large amount of detrital zircon U-Pb and muscovite  $^{40}\text{Ar}/^{39}\text{Ar}$  ages [16,21,24–26] from its trunk and Major tributaries.

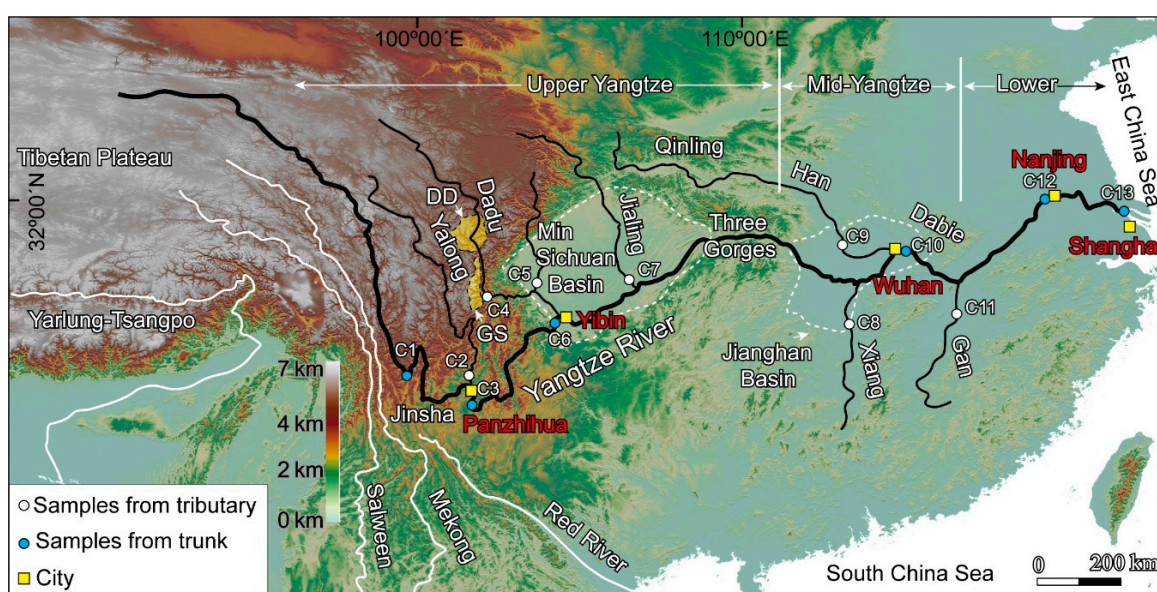


**Figure 1.** A schematic Map showing the drainage basin, sampling locations and Main distributaries of the Yangtze River. Sample locations of Major tributaries are shown as open circles. Samples from the Main trunk are shown as filled blue circles. The yellow shadow areas represent the Danba dome (DD) and Gongga shan (GS).

In this study, we combine previously reported detrital zircon U-Pb and muscovite  $^{40}\text{Ar}/^{39}\text{Ar}$  data derived from equivalent sampling points along the Yangtze River with the objective to take interpretation beyond the outcome of the individual samples. The comparison of detrital ages from the Yangtze River between muscovite and zircon shows different aspects of the provenance information. We focus on assessing the factors that control differences between data types. These factors should be considered in future sediment provenance studies using the two provenance tools.

## 2. Geological Setting

The Yangtze River is primarily situated in the Yangtze Block, surrounded by the Yidun Arc to the southwest, the Songpan-Garze Block to the west, the Qinling-Dabie orogen to the northwest and north and the Cathaysia Block to the east (Figure 2). The catchment drains a variety of rocks, including Archean and Proterozoic metamorphic and igneous rocks, Paleozoic carbonate, Mesozoic-Cenozoic igneous and siliciclastic rocks, and Quaternary sediments [27].

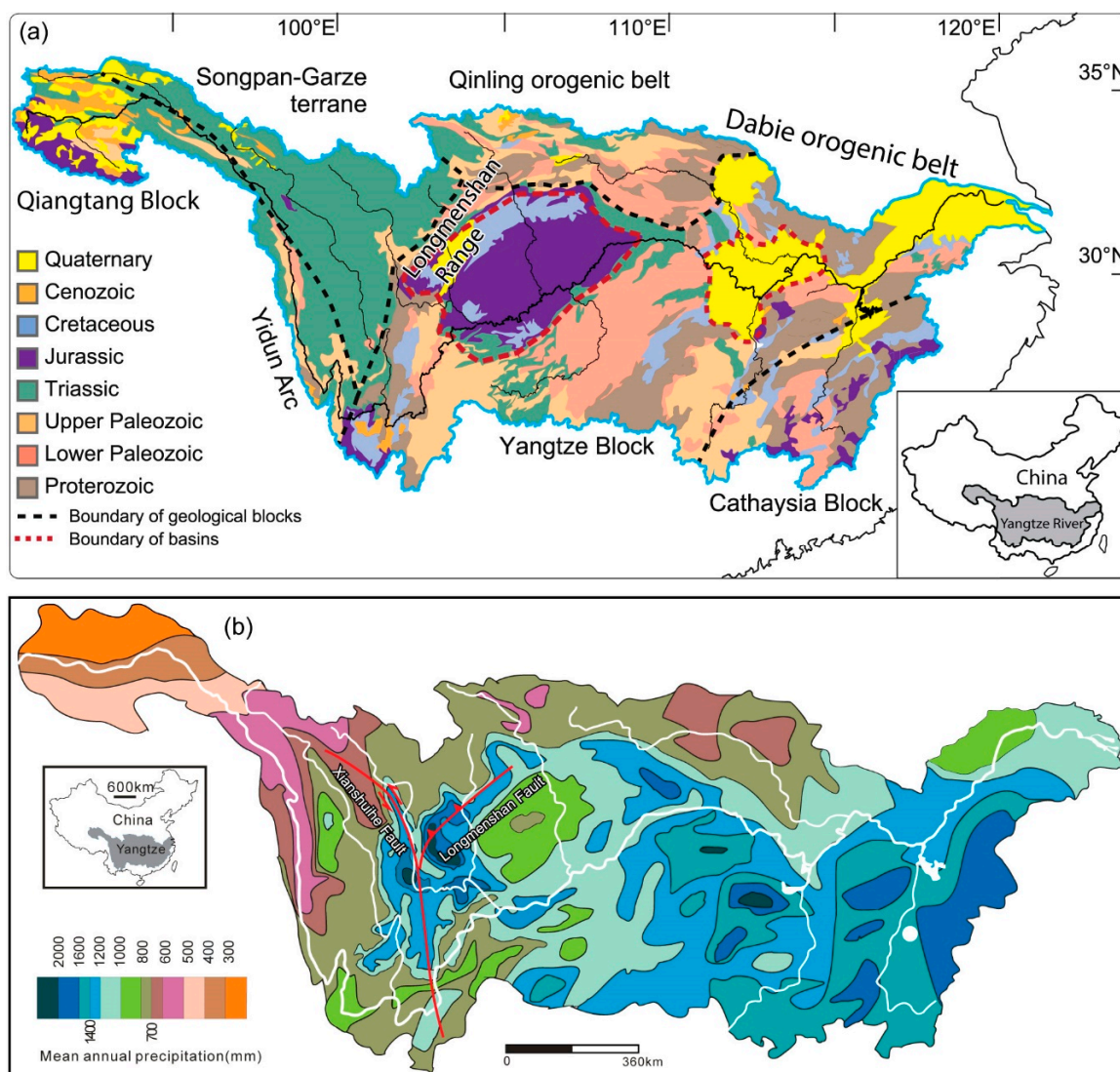


**Figure 2.** Generalized geological Map (a) (Modified from Saito et al. [28]) and the mean annual precipitation distribution of the Yangtze River (b). The mean annual precipitation distribution Map modified from Sun et al. [24].

The Major tributaries of the Yangtze River are characterized by different tectonic settings and bedrocks in their respective hinterlands (Figure 2a). From upstream to downstream the Main tributaries and their catchment areas include: (1) The Jinsha River basin, comprising Triassic low-grade metamorphic rocks, Paleozoic carbonate, and clastic and volcanic rocks [29,30]. (2) The Yalong, Min, and Dadu rivers draining the Songpan-Garze Block, which is composed of deformed and locally metamorphosed Triassic turbiditic sedimentary rocks [31,32]. (3) The upper Jialing River drainage area belongs to the South Qinling orogenic belt (Figure 2a), consisting of weakly metamorphosed Meso–Neoproterozoic basement. The central to southeastern Sichuan Basin is drained by the mid-lower Jialing River, where Jurassic–Cretaceous sandstone and mudstone is exposed. (4) The Han River basin in the Qinling orogenic belt is characterized by Neoproterozoic basement and Neoproterozoic–Devonian sediments, and early Paleozoic metamorphic rocks [33]. (5) The Xiang River belong to the Yangtze Block, containing mostly Proterozoic medium-low grade metamorphic and Cambrian and Ordovician carbonate rocks, and Jurassic–Quaternary terrestrial sediments [34]. (6) The Gan River is located in the Cathaysia Block, which is composed of Neoproterozoic conglomerate and sandstone, Jurassic granite, and Quaternary clastic sediments (Figure 2a).

### 3. Data Sets

We compiled and published data sets of zircon U-Pb ages from He et al. [21] and Yang et al. [26] and of muscovite  $^{40}\text{Ar}/^{39}\text{Ar}$  ages from Sun et al. [16,24,35] and Hoang et al. [25]. Available data cover the Main tributaries of the Yangtze River, including Yalong, Dadu, Min, Jialing, Xiang, Han, and Gan rivers (Figure 1). Six samples are from the trunk of the Yangtze River near Nanjing, Wuhan, Yibin, Panzhihua, and Shanghai cities. More than 91 zircon ages are available for each sample, ensuring with 95% certainty that no fraction greater than 6% was missed from the underlying detrital population [36]. For muscovite, 30–62 analyses per sample ensure a 95% certainty that no fraction greater than 15% was missed [36]. In total, 2557 zircon and 581 muscovite ages were compiled for discussion. All samples were collected from channel deposits. Samples are riverbed sand at least from two locations at each sample site to avoid bias on age distributions caused by hydraulic sorting [16,21,24]. Details of muscovite  $^{40}\text{Ar}/^{39}\text{Ar}$  age determinations are given in Sun et al. [16,24,35] and Hoang et al. [25]. Details of zircon U-Pb age determinations are described in He et al. [21] and Yang et al. [26].

### 4. Results

#### 4.1. Detrital Zircon

The detrital zircon U-Pb ages of 13 samples are presented in Figures 3b and 4a. Detrital zircon ages define a wide spectrum ranging from ~30 to 3200 Ma. Samples (C1, C3, and C6) from the Jinsha River have five Major age populations, i.e., 2.2–2.6 Ga, 1.5–2.0 Ga, 600–1000 Ma, 300–450 Ma, and 160–300 Ma (Figure 4a-1,-3,-4). For the Major tributaries (Yalong, Dadu and Min) in the upper Yangtze River, two age peaks (100–300 Ma and 600–1000 Ma) are displayed (Figure 4a-2,-5,-6). Four Major age peaks are present in the Jialing River (100–400 Ma, 700–1200 Ma, 1.5–2.0 Ga and 2.2–2.6 Ga) (Figure 4a-7). For the midstream segment, five age peaks are displayed in the Mainstream (2.2–2.6 Ga, 1.5–2.0 Ga, 700–1000 Ma, 300–600 Ma, and 200–300 Ma), which is similar to ranges of ages seen in the upper Yangtze.

#### 4.2. Detrital Muscovite

In the upper Yangtze, three samples from the Jinsha River show a dominant muscovite age peak at ~250 Ma (Figure 4b-1,-3,-4). Forty muscovite grains from the Yalong River show a dominant age peak at ~810 Ma and a minor peak at ~230 Ma (Figure 4b-2). All dated muscovite grains of the Dadu River are younger than 160 Ma, with a Major muscovite age peak younger than 60 Ma (Figure 4b-5). Muscovite grains from the Min River are dominated by muscovite ages between 80–200 Ma, with a Major peak around 180 Ma (Figure 4b-6). The muscovite grains from the Jialing River show a range from 190 to 300 Ma, with a prominent peak at ~208 Ma (Figure 4b-7). In the mid-lower Yangtze tributaries (Han, Xiang and Gan), most of muscovite ages fall into an age range of 100–300 Ma (Figure 4b-8,-9,-11). None of these grains are younger than 60 Ma. The three modern Yangtze trunk sediments (C10, C12, and C13) yield similar muscovite age distributions (Figure 4b-10,-12,-13). Most of the muscovite grains in samples C10, C12, and C13 are younger than 100 Ma, accounting for ~71%, ~67%, and ~53% of the total dated grains of each sample. These young muscovite ages overlap with the Dadu River provenance pattern (Figure 4b-5,-10,-12,-13).

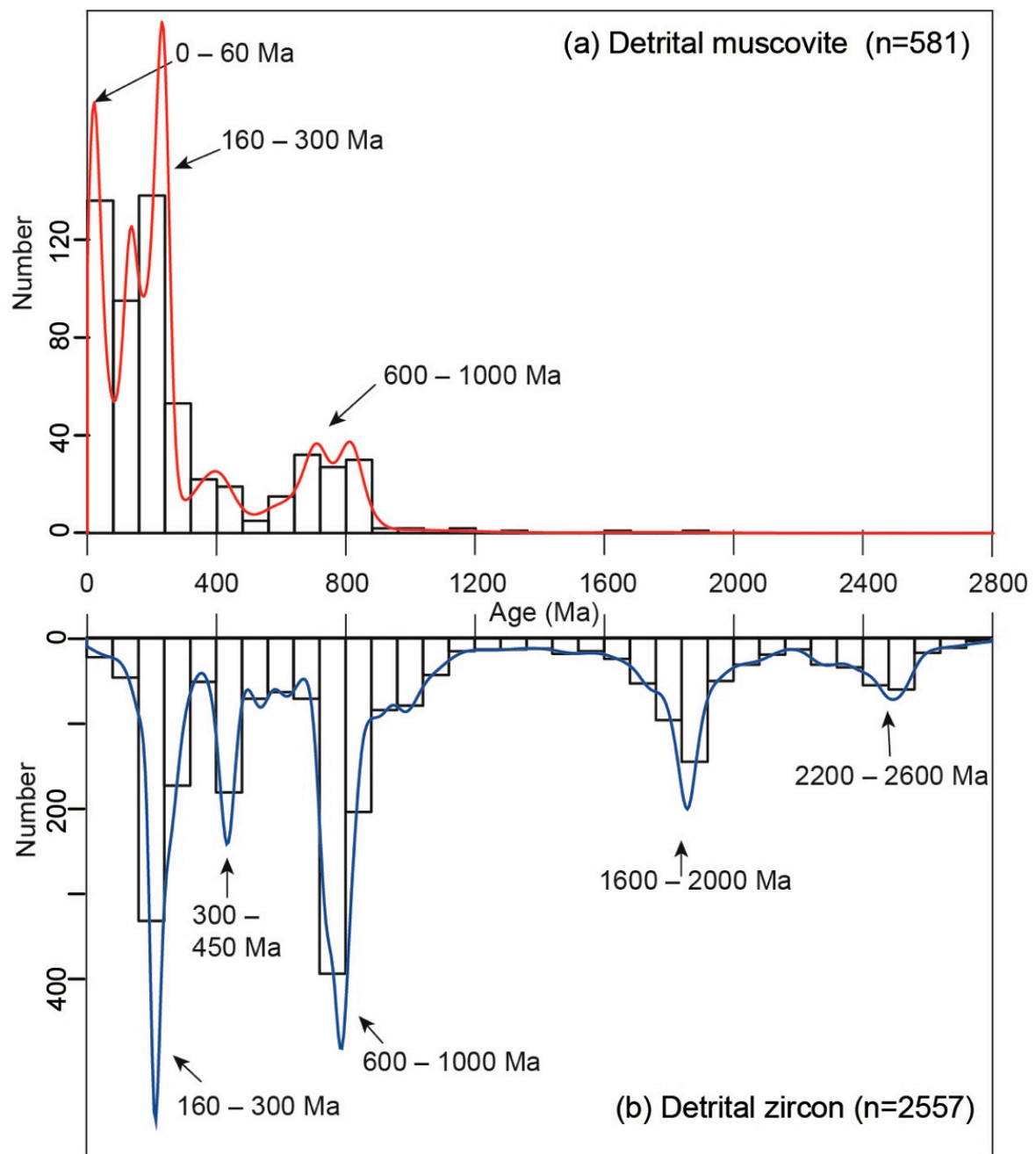


**Figure 3.** Probability density diagrams for pooled detrital muscovite  $^{40}\text{Ar}/^{39}\text{Ar}$  (a) and zircon U-Pb (b) ages of the Yangtze River basin. Detrital zircon data from He et al. [21] and Yang et al. [26]. Detrital muscovite data from Sun et al. [16,24,35] and Hoang et al. [25].

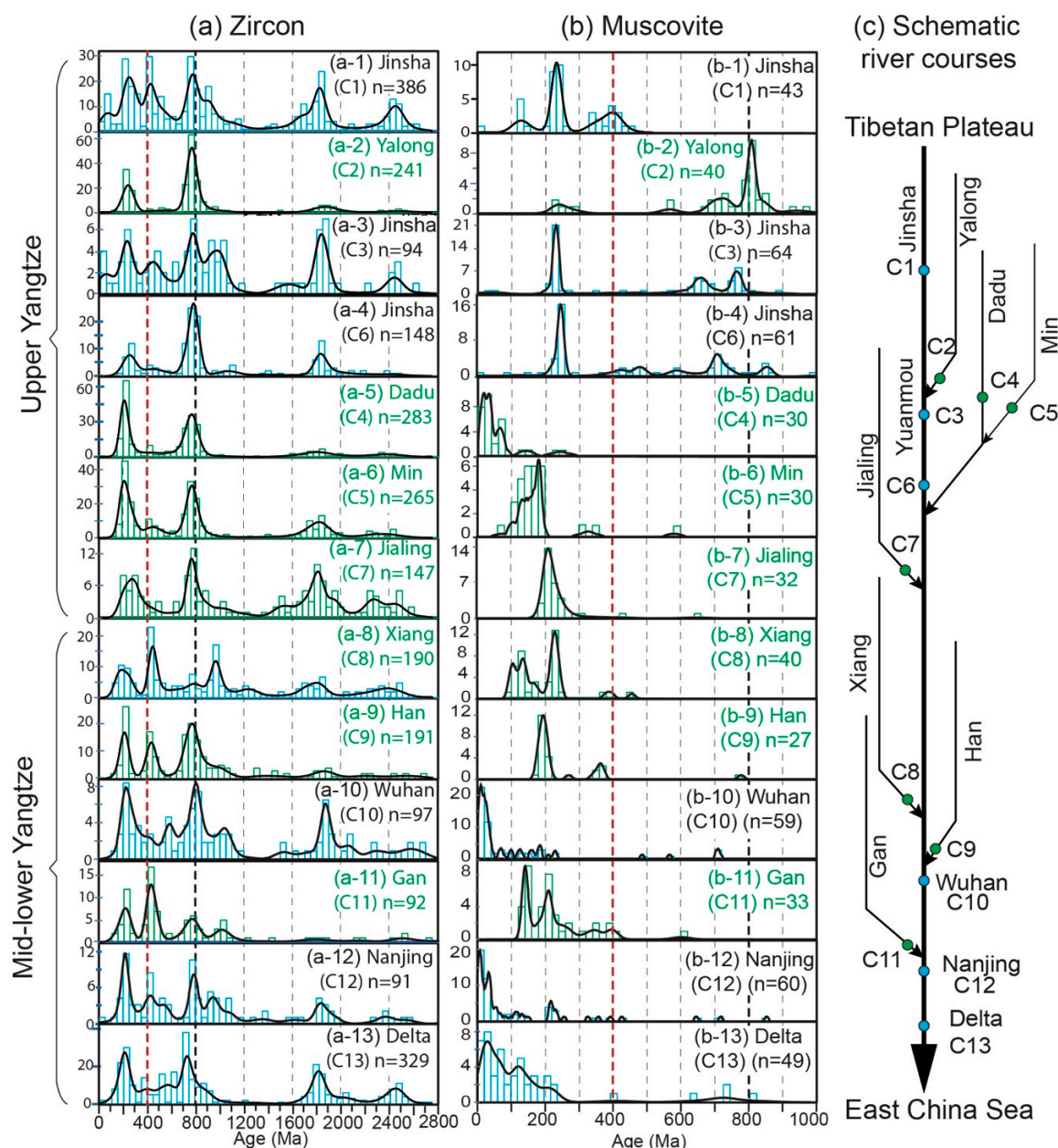


**Figure 4.** Comparison of age distributions between detrital zircons (a) and muscovites (b) of modern sands of the Yangtze. (c) Schematic river course of the Yangtze. Note the difference in age scale between muscovite (0–1000 Ma) and zircon (0–2800 Ma). The dashed vertical red and black lines Mark 400 and 800 Ma, respectively. The histogram diagrams in blue and green are samples from the Main stream and Major tributaries, respectively. Detrital zircon data from He et al. [21] and Yang et al. [26]. Detrital muscovite data from Sun et al. [16,24] and Hoang et al. [25].

## 5. Discussion

### 5.1. Comparison of Detrital Muscovite and Zircon Ages

#### 5.1.1. Comparison of Pooled Age Distributions

In order to assess the general differences in age distribution between detrital muscovites and zircons of the Yangtze River, the muscovite and zircon ages of modern Yangtze sands are pooled and presented in Figure 3. The Major five zircon age peaks (2.2–2.6 Ga, 1.6–2.0 Ga, 600–1000 Ma,

300–450 Ma, and 160–300 Ma) correspond to Major granitoid Magmatic events within the Yangtze River basin [21]. The age distributions of muscovite and zircon are different in the following two aspects: (1) Muscovite grains are lacking in age populations at 1600–2000 Ma and 2200–2600 Ma recorded by detrital zircons. (2) The height of muscovite age peaks at 0–60 Ma, 160–300 Ma, and 600–1000 Ma are different from zircon age peaks in relative probability and number.

### 5.1.2. Comparison of Major Tributaries with Main Trunk of the Yangtze

The variation in muscovite and zircon age distributions from upstream to downstream in the Yangtze River systems allow us to better understand the Major sediment contributors to the lower Yangtze. The comparison of age distributions between detrital muscovite and zircon grains (Figure 4) shows the following two differences: (1) The Major zircon age peaks (2.2–2.6 Ga, 1.6–2.0 Ga, 600–1000 Ma, 300–450 Ma, and 160–300 Ma, Figures 3b and 4a) can be observed in all trunk samples, but the three Major muscovite age peaks (600–1000 Ma, 160–250 Ma, and 0–60 Ma, Figures 3a and 4b) are not always identified in the trunk samples. (2) The concentration of Cenozoic muscovite grains (>40%) is pronouncedly increased for trunk samples in the mid-lower reaches (C10, C12, and C13), but the detrital zircon age distributions of trunk samples do not significantly change toward lower reaches.

Cenozoic muscovite grains in the mid-lower reaches (JC10, CJ12, and C13) probably were derived from the Dadu River in the upper reaches because Cenozoic muscovites are only present in the Dadu River among all sampled tributaries. This suggests that the Dadu River in the upper reaches is an important muscovite contributor to the sediment of the lower reaches. The reported Cenozoic muscovite  $^{40}\text{Ar}/^{39}\text{Ar}$  ages in the Dadu River basin are from the Gongga shan (3.5–12.1 Ma, [37]) and Danba dome (35.1–104.3 Ma, [38]) (see Figure 1 for location). Therefore, most of the Cenozoic muscovite grains in the lower Yangtze were derived from only these two regions. In contrast, the zircon age distributions show a different picture. Using multiple detrital zircon U-Pb age distribution comparison techniques and a distribution-mixing model, Wissink et al. [6] suggest that the Yalong, Dadu, and Min rivers are the Major sediment contributors to the lower Yangtze.

Main trunk samples (C10, CJ12, and C13) from the mid-lower reaches contain more than 40% Cenozoic muscovite grains which were derived from the Dadu River. It could be argued that the Dadu River cannot supply more than 40% muscovite grains to mid-lower Yangtze because this river is not a dominant water supplier to mid-lower Yangtze. However, the Dadu River drains the Xianshui He Fault area that has already been tectonically active since the Miocene (Figure 2b) [37]. This region experiences strong precipitation and is expected to facilitate more landslides and intense erosion (Figure 2b) and thus water and sediment budgets may be decoupled. Moreover, the exhumation rates of the Xianshui He Fault area inferred from the thermochronometry data are higher than other areas of the upper Yangtze River [39–41]. In addition, Cook et al. [42] report millennial erosion rates based on detrital  $^{10}\text{Be}$  data in the Gongga shan of >5 mm/year. Erosion rates increase from west to east more than one hundred-fold from 0.013–0.04 mm/year in the upper Jinsha River to >5 mm/year in the Dadu River basin [42,43].

### 5.2. Factors Related to the Difference in Zircon and Muscovite Signals

To correctly interpret provenance data, we need to understand, which geochronometer or provenance tools best reflects sediment provenance and under what circumstances (e.g., in complex orogens). We argue that the differences in provenance signal between muscovite and zircon could be caused by the following six factors: (1) lithological effect; (2) mineral abundance; (3) dilution of the mid-lower reaches; (4) differences in closure temperature; (5) differences in resistance to weathering; and (6) laser spot location on zircons.

- (1) In Figure 4, in some rivers we note remarkable differences in age distributions: For example in the Dadu River we note high abundance of young muscovite ages without an equivalent population of young zircon ages, whereas, in the Jinsha River we see the reverse, young zircon ages that

do not have a complement of young muscovite  $^{40}\text{Ar}/^{39}\text{Ar}$  ages. Such discrepancies point to a lithological effect: Young volcanics and young I-type granites will add a zircon signal to the sediment [44], but because these rock types are generally free of white mica, an equivalent signal in the muscovite population is lacking. Conversely, when we see a young muscovite age signal in the sediment without an equivalent zircon age population, the source rock of the sediment is likely to be more consistent with low to medium grade metamorphic basement where muscovite is abundant, but as the metamorphic grade is too low for zircon crystallization an equivalent age signal in the zircon data will be lacking. This implies that the choice of used provenance tools should depend on the geological composition of the hinterland.

- (2) To assess if mineral abundance in the Major tributaries of the Yangtze River causes the dominance of the Dadu River muscovites in the lower Yangtze, we compiled mineral fertility data (mica and zircon) from Vezzoli et al. [45]. Figure 5 shows that the concentration of mica in modern sediment of the Dadu River is much lower than that of the Han River and higher than the Jialing and Jinsha rivers. However, comparison of muscovite age distribution between the Han River and delta (Figure 4b-9,-13) suggests that the Han River is not Major muscovite supplier to the lower Yangtze. The zircon concentration of the Gan and Xiang rivers in the middle reaches are higher than other tributaries. These two rivers are not the Major zircon contributors to the lower reaches. Therefore, we can rule out large concentration variation in mica in the sediment as being a Major control on the dominance of the Dadu River muscovites in the lower reaches.

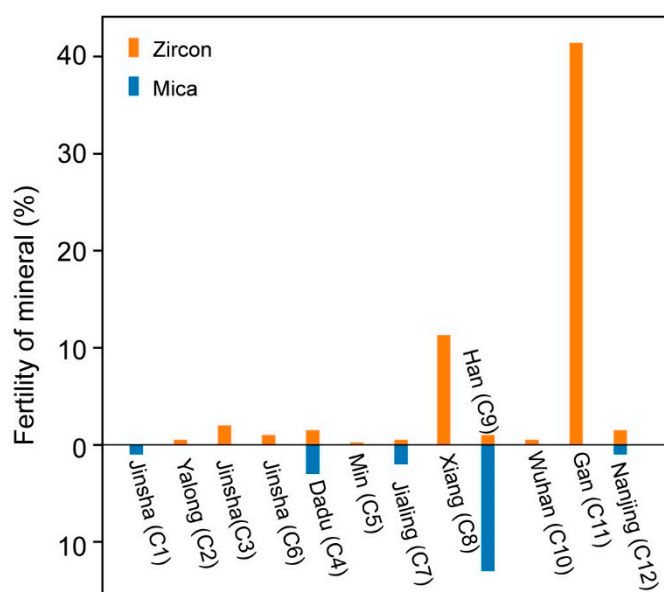


**Figure 5.** Zircon and mica fertility of Major tributaries. Concentration of zircon grains in the heavy mineral fraction. Mica and zircon data from Vezzoli et al. [45].

- (3) The sediment from the upper Yangtze is potentially diluted by sediment from the tributaries in the mid-lower reaches. The effect of this dilution on differences between muscovite and zircon age distributions should be considered. The concentration of Cenozoic muscovite grains (>40%) in trunk samples pronouncedly increased in the mid-lower reaches (C10, C12, and C13), but the detrital zircon age distributions of trunk samples do not significantly change toward lower reaches. The detrital muscovite ages of the Major tributaries in the mid-lower reaches fall into two age peaks at 100–160 Ma and 180–260 Ma. The two Major age populations are minor in samples near Wuhan (C10), Nanjing (C12), and delta (C13). This suggests that the Cenozoic muscovite signals of the Dadu River, that is relatively far upstream (Figure 4c), is not significantly affected by the dilution of the mid-lower reaches (Han, Xiang, and Gan rivers). Moreover,

the 1500–2000 Ma zircon age peak of the Main trunk (samples C10, C12, and C13) in the mid-lower reaches is much higher than the tributaries (samples C8, C9, and C11) (Figure 4a-10,-12,-13), implying that the effect of dilution of zircons from the mid-lower reaches is also limited. We therefore suggest that the dilution of mid-lower reaches is limited in terms of the muscovite and zircon age signals.

- (4) The closure temperature is the temperature at which muscovite  $^{40}\text{Ar}/^{39}\text{Ar}$  or zircon U-Pb systems have cooled so that there is no longer any significant diffusion of the parent and daughter isotopes out of system. The closure temperature of muscovite (350–425 °C, [12,46]) is much lower than zircon (>900 °C, [13]). The zircon U-Pb age gives the crystallization or high-grade metamorphism and the muscovite  $^{40}\text{Ar}/^{39}\text{Ar}$  age is age imparted as terrain cooled through closure temperature. Figure 3a shows that the detrital muscovite grains from the Yangtze are absent of older (>1000 Ma) age peaks, which could be caused by muscovite's lower closure temperature. Potentially older (>1000 Ma) muscovite grains in the Yangtze River could have been reset by younger tectonic events.
- (5) The absence of older (>1000 Ma) muscovite grains in the Yangtze River also could be caused by abrasion and chemical dissolution during weathering and transport in multiple phases of sediment recycling. Muscovites in the Triassic Songpan-Garze flysch deposits in the upper Yangtze River have experienced multiple recycling. Previous studies suggest that the detritus in these areas is derived from Paleozoic and pre-Cambrian crystalline and sedimentary rocks of the Qinling-Dabie orogen and South China Block [47–50]. Detrital zircon U-Pb and Hf isotopic data of the Mesozoic sediment in basins of the South China Block (Pingle, Jiangnan, and Sichuan basins) also suggest derivation of sediments from the Cathaysia Block [51]. Therefore, current Yangtze sands have experienced complex multiple erosion, transport and deposition processes that may have led to a reduction in size and abundance of the older grains. Detrital muscovite grains from the Yangtze River only record age populations of 600–1000 Ma, 160–300 Ma, and 0–60 Ma and lack older populations (2000–2500 Ma and 1600–2000 Ma) (Figure 3a). The absence of the two older age components probably results from muscovite's lower resistance to physical and chemical weathering when compared with zircon. The weathering has either completely destroyed the grain or reduced the grain size down to less than 200  $\mu\text{m}$ , which are not selected for age analyses in this study.
- (6) The differences in age distribution between zircon and muscovite also could be caused by laser spot location targeted for U-Pb analysis. Owing to the low solubility of zircon in hydrous granitoid melt, zircons can survive anatexis event [11]. Many zircon crystals are zoned with cores reflecting the ages of much older protoliths, which are universally referred to as the inherited component in the zircon population. However,  $^{40}\text{Ar}/^{39}\text{Ar}$  in muscovite in general record only the later, post-peak cooling history. The apparent age of muscovite  $^{40}\text{Ar}/^{39}\text{Ar}$  age system is generally younger than zircon U-Pb system for metamorphic or magmatic rocks. Muscovite detrital data of trunk samples from the mid-lower reaches suggest that the Gongga shan and Danba dome in the Dadu River basin are two important sediment suppliers to the mid-lower reaches. Unsurprisingly, zircons in the Gongga shan and Danba dome show complex core rim texture (Figure 6c,d). Figure 6c shows that almost all Cenozoic ages are recorded by rims of dated zircons from the Gongga shan. This suggests that the narrow rims grew around the older core during Cenozoic intrusion ((1), (2), and (3) in Figure 6a). The Cenozoic ages recorded by rims of zircons also recorded by the bedrock muscovite  $^{40}\text{Ar}/^{39}\text{Ar}$  ages [37] (Figure 6a). The Danba dome has undergone Barrovian type metamorphism at 200–180 Ma. Zircon growth at low metamorphic grades is minimal ((4) in Figure 6a). In the kyanite and sillimanite zones, narrow zircon growth has been observed in the Danba dome [52]. Therefore, rims of zircons from the Danba dome and Gongga shan are unlikely to be detected in the detrital record, due to laser spot location targeting on core and also the high likelihood that abrasion during transport will remove thin rims. Figure 4a-5 shows that the Cenozoic ages are not detected by the detrital zircons from the Dadu River near the Gongga shan

(sample C4). Figure 6b presents that the cores of detrital zircons from the modern Yangtze sands are always chosen as laser spot position instead of the narrow rims. Combination with dilution of sediment from the tributaries in the mid-lower reaches, the Cenozoic ages of the Gongga shan and Danba dome are not detected by detrital zircon in the mid-lower Yangtze River like muscovites.

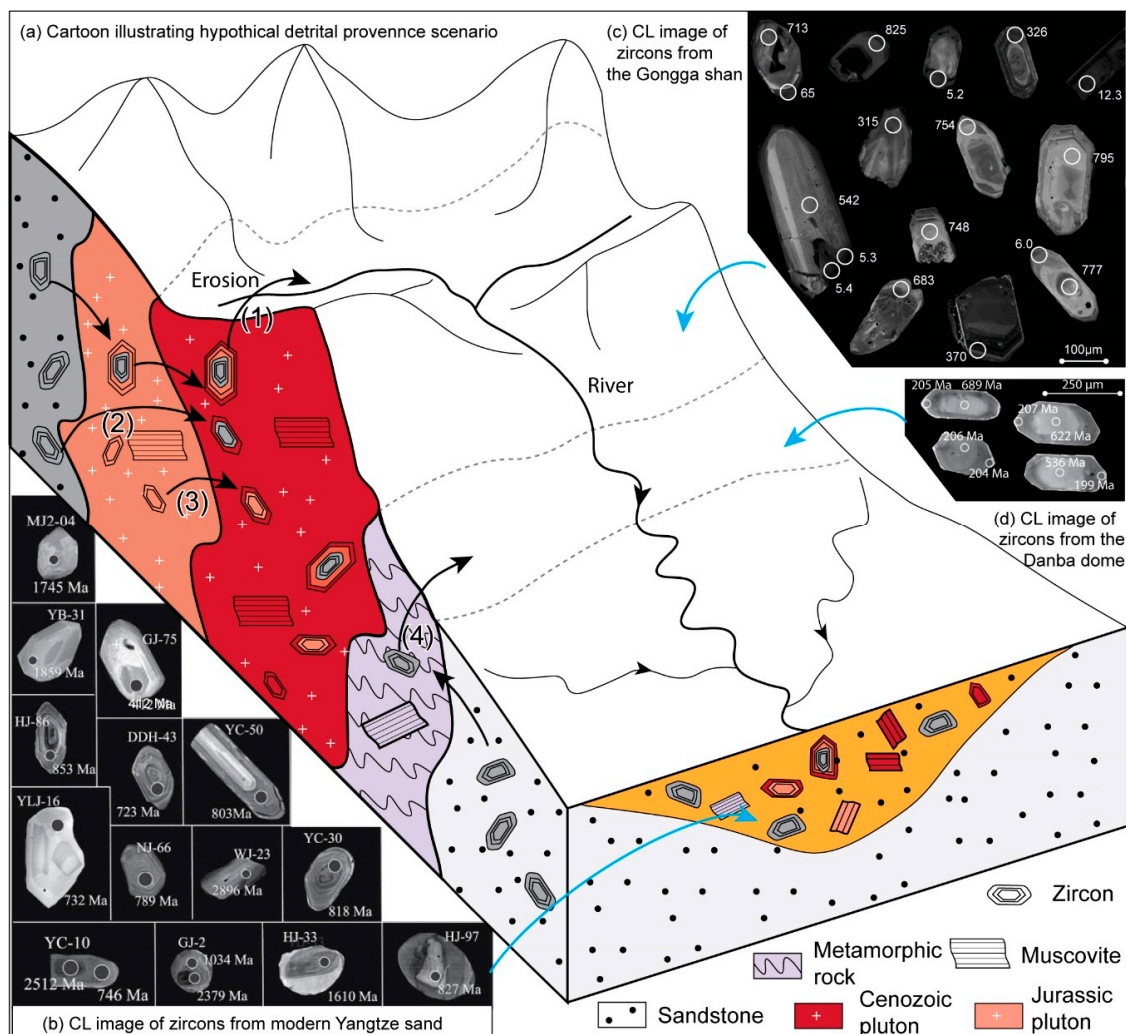


**Figure 6.** A cartoon showing the possible reasons for lack Cenozoic zircon in the lower reaches of the Yangtze (a). (1) Indicates detrital zircons experienced two phases of overgrowth. (2) Indicates overgrowth of detrital zircons in the Cenozoic. Magmatic zircon overgrowth in the Cenozoic (3). (4) Indicates no wide overgrowth of detrital zircon in the low-degrade metamorphism. Note that muscovite Ar system cannot survive Magmatic or metamorphic events. (b) Cathodoluminescence images of detrital zircons from the Yangtze River. Images are from He et al. [21]. (c,d) Cathodoluminescence images of dated zircons from the Gongga shan and Danba dome, respectively. Zircon images of the Gongga shan are from Robert et al. [53]. Zircon images of the Danba dome are from Jolivet et al. [52].

### 5.3. Implications

The lithological effect on provenance study using detrital mineral ages (e.g., muscovite or zircon) could be reduced by the following two approaches: (1) Carrying out high-resolution petrographic and heavy-mineral analyses. Petrographic and mineralogical data of sediment could provide information for selecting provenance tool (e.g., fertility of target mineral). (2) Applying multi-proxy provenance approach. Multiple chemical and isotopic indicators of single mineral grains can extract more robust

information about sediment provenance. Sediment signals missed in one mineral could be detected by other minerals. As we have shown in this study, the Cenozoic signal detected by muscovite grains is missing in zircon ages in the Dadu River. Similarly, the Cenozoic zircon ages in the Jinsha River is not detected by muscovite  $^{40}\text{Ar}/^{39}\text{Ar}$  ages. By combining multiple-proxies approaches, an increased understanding can be obtained of sediment provenance.

The comparison of muscovite and zircon ages suggests that detrital zircons in the Yangtze sediment experienced multiple cycles of deposition and erosion due to its high closure temperature and resistance to weathering. Possibility of zircon reworking should be considered for provenance interpretation. The following four approaches have been used to identify zircon reworking: (1) Direct field observation (e.g., appearance of sandstone gravels) [35]. (2) Time-transgressive similarities in detrital zircon age distribution, especially in old age populations [54]. (3) Supplementary information from other detrital minerals (e.g., apatite fission track ages [55]). (4) He-Pb double dating of detrital zircons [56].

In the case of Magmatic zircons in the Gongga shan, rim overgrowths are typically autocrusts linked to last-stage growth corresponding to crystallization from the final pulses of Magma [53] (Figure 6a). U-Pb rim ages of detrital zircons record the last zircon-forming tectonothermal event in the original source rock, while core ages record inheritance from the local country rocks or co-genetic Magmatic ages derived from earlier melt pulses in the Magma plumbing system [57]. In the Yangtze River, detrital zircon U-Pb dating is widely used to reconstruct evolution of this river in the previous studies [17,18,58–67]. However, no consensus exists on when and how the present drainage pattern formed based on detrital zircon data from various basins. The laser spot positions on rims or cores of zircons are often randomly selected for U-Pb dating. The most important evidence for reconstruction the development of the Yangtze River is the presence of sediment signal from present upper Yangtze River in the ancient Yangtze sediment. Just like the case of modern Yangtze sands in this study, the characteristic Cenozoic signal of the upper Yangtze is difficult to be detected in the ancient sediment in the mid-lower Yangtze using the randomly selecting strategy. By increasing the number of analyses, the chance of detecting Cenozoic signal of the upper Yangtze could be increased. Alternatively, by increasing the number of laser spot on rims of detrital zircons, the characteristic Cenozoic signal of the upper Yangtze could be enhanced. Additionally, multiple isotopic indicators (e.g., detrital mineral  $^{40}\text{Ar}/^{39}\text{Ar}$  dating and apatite and rutile U-Pb) of single mineral grains could provide complementary information.

## 6. Conclusions

In order to reveal factors controlling the difference in age distributions between muscovite and zircon of same sample, we compared published datasets of detrital muscovite  $^{40}\text{Ar}/^{39}\text{Ar}$  and zircon U-Pb ages of modern sands from the Yangtze River. The comparison of pooled age distributions between muscovite and zircon presents that muscovite grains are absent of age populations of 2000–2500 Ma and 1600–2000 Ma, suggesting that zircons in the Yangtze River experienced multiple cycles of erosion and deposition. The detrital muscovite ages of each sample were also compared with corresponding detrital zircon ages. Detrital muscovite ages imply that the Dadu River in the upper Yangtze is an important sediment supplier to the lower Yangtze. However, detrital zircon data suggest that the Yalong, Dadu, and Min rivers are the Major sediment contributors to the lower reaches. These differences could be caused by discrepancies in closure temperature and durability and potentially differences in source rock contributing to the sediment in each of these river branches. In order to reconstruct the development of the Yangtze using detrital U-Pb analysis, increasing the number of analyzed zircon rims is potentially a way to enhance the characteristic sediment signal of the upper Yangtze.

**Author Contributions:** For research articles with several authors, a short paragraph specifying their individual contributions must be provided. The following statements should be used “Conceptualization, X.S. and J.R.W.; methodology, K.F.K.; formal analysis, X.S.; writing—original draft preparation, X.S., K.F.K.; writing—review and editing, Y.T. and Z.Z.; funding acquisition, J.R.W., K.F.K., Y.T. and C.L.”, please turn to the CRediT taxonomy for the term explanation. Authorship must be limited to those who have contributed substantially to the work reported. All authors have read and agreed to the published version of the manuscript.

**Funding:** This study is financially supported by the National Natural Science Foundation of China (41671011, 41672355, 41888101, and 41801003) and the Fundamental Research Funds for the Central Universities (19lgpy72). K.F.K. is supported by NWO-ALW grant 864.12.005.

**Acknowledgments:** This work was supported by the argon geochronology laboratory of the Vrije Universiteit Amsterdam.

**Conflicts of Interest:** The authors declare no conflict of interest.

## References

1. Copeland, P. On the use of geochronology of detrital grains in determining the time of deposition of clastic sedimentary strata. *Basin Res.* **2020**. [[CrossRef](#)]
2. Dickinson, W.R.; Gehrels, G.E. Use of U–Pb ages of detrital zircons to infer Maximum depositional ages of strata: A test against a Colorado Plateau Mesozoic database. *Earth Planet. Sci. Lett.* **2009**, *288*, 115–125. [[CrossRef](#)]
3. Coutts, D.S.; Matthews, W.A.; Hubbard, S.M. Assessment of widely used methods to derive depositional ages from detrital zircon populations. *Geosci. Front.* **2019**, *10*, 1421–1435. [[CrossRef](#)]
4. Fedo, C.M.; Sircombe, K.N.; Rainbird, R.H. Detrital zircon analysis of the sedimentary record. *Rev. Mineral. Geochem.* **2003**, *53*, 277–303. [[CrossRef](#)]
5. He, M.; Zheng, H.; Bookhagen, B.; Clift, P.D. Controls on erosion intensity in the Yangtze River basin tracked by U–Pb detrital zircon dating. *Earth Sci. Rev.* **2014**, *136*, 121–140. [[CrossRef](#)]
6. Wissink, G.K.; Hoke, G.D. Eastern Margin of Tibet supplies most sediment to the Yangtze River. *Lithosphere* **2016**. [[CrossRef](#)]
7. Gehrels, G. Detrital zircon U–Pb geochronology applied to tectonics. *Annu. Rev. Earth Planet. Sci.* **2014**, *42*, 127–149. [[CrossRef](#)]
8. Najman, Y. The detrital record of orogenesis: A review of approaches and techniques used in the Himalayan sedimentary basins. *Earth Sci. Rev.* **2006**, *74*, 1–72. [[CrossRef](#)]
9. Zhu, G.; Wang, Y.S.; Wang, W.; Zhang, S.; Liu, C.; Gu, C.C.; Li, Y.J. An accreted micro-continent in the north of the Dabie Orogen, East China: Evidence from detrital zircon dating. *Tectonophysics* **2017**, *698*, 47–64. [[CrossRef](#)]
10. Haines, P.W.; Turner, S.P.; Kelley, S.P.; Wartho, J.A.; Sherlock, S.C.  $^{40}\text{Ar}/^{39}\text{Ar}$  dating of detrital muscovite in provenance investigations: A case study from the Adelaide Rift Complex, South Australia. *Earth Planet. Sci. Lett.* **2004**, *227*, 297–311. [[CrossRef](#)]
11. Miller, J.S.; Matzel, J.E.P.; Miller, C.F.; Burgess, S.D.; Miller, R.B. Zircon growth and recycling during the assembly of large, composite arc plutons. *J. Volcanol. Geotherm. Res.* **2007**, *167*, 282–299. [[CrossRef](#)]
12. Harrison, T.M.; Célérier, J.; Aikman, A.B.; Hermann, J.; Heizler, M.T. Diffusion of  $^{40}\text{Ar}$  in muscovite. *Geochim. Cosmochim. Acta* **2009**, *73*, 1039–1051. [[CrossRef](#)]
13. Lee, J.K.W.; Williams, I.S.; Ellis, D.J. Pb, U and Th diffusion in natural zircon. *Nature* **1997**, *390*, 159–162. [[CrossRef](#)]
14. Garzanti, E.; Vermeesch, P.; Andò, S.; Vezzoli, G.; Valagussa, M.; Allen, K.; Kadi, K.A.; Al-Juboury, A.I.A. Provenance and recycling of Arabian desert sand. *Earth Sci. Rev.* **2013**, *120*, 1–19. [[CrossRef](#)]
15. Thomas, W.A. Detrital-zircon geochronology and sedimentary provenance. *Lithosphere* **2011**, *3*, 304–308. [[CrossRef](#)]
16. Sun, X.L.; Li, C.A.; Kuiper, K.F.; Wang, J.T.; Tian, Y.T.; Vermeesch, P.; Zhang, Z.J.; Zhao, J.X.; Wijbrans, J.R. Geochronology of detrital muscovite and zircon constrains the sediment provenance changes in the Yangtze River during the late Cenozoic. *Basin Res.* **2018**, *30*, 636–649. [[CrossRef](#)]
17. Jia, J.T.; Zheng, H.B.; Huang, X.T.; Wu, F.Y.; Yang, S.Y.; Wang, K.; He, M.Y. Detrital zircon U–Pb ages of late cenozoic sediments from the Yangtze delta: Implication for the evolution of the Yangtze River. *Chin. Sci. Bull.* **2010**, *55*, 1520–1528. [[CrossRef](#)]
18. Wang, J.T.; Li, C.A.; Yang, Y.; Shao, L. Detrital zircon geochronology and provenance of core sediments in zhoulao town, Jiangnan Plain, China. *J. Earth Sci.* **2010**, *21*, 257–271. [[CrossRef](#)]
19. Yang, S.Y.; Wang, Z.B.; Guo, Y.; Li, C.X.; Cai, J.G. Heavy mineral compositions of the Changjiang (Yangtze River) sediments and their provenance-tracing implication. *J. Asian Earth Sci.* **2009**, *35*, 56–65. [[CrossRef](#)]

20. Zhang, Z.J.; Tyrrell, S.; Li, C.A.; Daly, J.S.; Sun, X.L.; Blowick, A.; Lin, X. Provenance of detrital K-feldspar in Jiangnan Basin sheds new light on the Pliocene–Pleistocene evolution of the Yangtze River. *Geol. Soc. Am. Bull.* **2016**, *128*, B31445.1. [[CrossRef](#)]
21. He, M.Y.; Zheng, H.B.; Clift, P.D. Zircon U–Pb geochronology and Hf isotope data from the Yangtze River sands: Implications for Major Magmatic events and crustal evolution in central China. *Chem. Geol.* **2013**, *360–361*, 186–203. [[CrossRef](#)]
22. Shao, L.; Li, C.A.; Yuan, S.Y.; Kang, C.G.; Wang, J.T.; Li, T. Neodymium isotopic variations of the late Cenozoic sediments in the Jiangnan Basin: Implications for sediment source and evolution of the Yangtze River. *J. Asian Earth Sci.* **2012**, *45*, 57–64. [[CrossRef](#)]
23. He, M.Y.; Zheng, H.B.; Huang, X.T.; Jia, J.T.; Li, L. Yangtze River sediments from source to sink traced with clay mineralogy. *J. Asian Earth Sci.* **2013**, *69*, 60–69. [[CrossRef](#)]
24. Sun, X.L.; Li, C.A.; Kuiper, K.F.; Zhang, Z.J.; Gao, J.H.; Wijbrans, J.R. Human impact on erosion patterns and sediment transport in the Yangtze River. *Glob. Planet. Chang.* **2016**, *143*, 88–99. [[CrossRef](#)]
25. Hoang, L.V.; Clift, P.D.; Mark, D.; Zheng, H.B.; Mai Thanh, T. Ar–Ar muscovite dating as a constraint on sediment provenance and erosion processes in the Red and Yangtze river systems, SE Asia. *Earth Planet. Sci. Lett.* **2010**, *295*, 379–389. [[CrossRef](#)]
26. Yang, S.Y.; Zhang, F.; Wang, Z.B. Grain size distribution and age population of detrital zircons from the Changjiang (Yangtze) River system, China. *Chem. Geol.* **2012**, *296–297*, 26–38. [[CrossRef](#)]
27. *Geological Map of China (1:2,500,000)*; China Geological Map Press: Beijing, China, 2004.
28. Saito, K.; Tada, R.; Zheng, H.B.; Irino, T.; Luo, C.; He, M.Y.; Wang, K.; Suzuki, Y. ESR signal intensity of quartz in the fine-silt fraction of riverbed sediments from the Yangtze River: A provenance tracer for suspended particulate Matter. *Prog. Earth Planet. Sci.* **2017**, *4*. [[CrossRef](#)]
29. Reid, A.J.; Wilson, C.J.L.; Phillips, D.; Liu, S. Mesozoic cooling across the Yidun Arc, central-eastern Tibetan plateau: A reconnaissance  $^{40}\text{Ar}/^{39}\text{Ar}$  study. *Tectonophysics* **2005**, *398*, 45–66. [[CrossRef](#)]
30. Wu, W.H.; Xu, S.J.; Yang, J.D.; Yin, H.W.; Tao, X.C. Sr fluxes and isotopic compositions in the headwaters of the Yangtze River, Tongtian River and Jinsha River originating from the Qinghai–Tibet Plateau. *Chem. Geol.* **2009**, *260*, 63–72. [[CrossRef](#)]
31. Roger, F.; Jolivet, M.; Malavieille, J. The tectonic evolution of the Songpan–Garze (north Tibet) and adjacent areas from proterozoic to present: A synthesis. *J. Asian Earth Sci.* **2010**, *39*, 254–269. [[CrossRef](#)]
32. Xu, Z.Q.; Hou, L.W.; Wang, Z.X.; Fu, X.F.; Huang, M.H. *Orogenic Processes of the Songpan–Garze Orogenic Belt of China*; Geological Publishing House: Beijing, China, 1992; pp. 1–235.
33. Dong, Y.P.; Zhang, G.W.; Neubauer, F.; Liu, X.M.; Genser, J.; Hauzenberger, C. Tectonic evolution of the Qinling orogen, China: Review and synthesis. *J. Asian Earth Sci.* **2011**, *41*, 213–237. [[CrossRef](#)]
34. Shu, L.S.; Faure, M.; Yu, J.H.; Jahn, B.M. Geochronological and geochemical features of the Cathaysia Block (South China): New evidence for the Neoproterozoic breakup of Rodinia. *Precambrian Res.* **2011**, *187*, 263–276. [[CrossRef](#)]
35. Sun, X.L.; Kuiper, K.F.; Tian, Y.T.; Li, C.A.; Zhang, Z.J.; Gemignani, L.; Guo, R.J.; de Breij, V.H.L.; Wijbrans, J.R.  $^{40}\text{Ar}/^{39}\text{Ar}$  mica dating of late Cenozoic sediments in SE Tibet: Implications for sediment recycling and drainage evolution. *J. Geol. Soc.* **2020**, *177*, 843–854. [[CrossRef](#)]
36. Vermeesch, P. How Many grains are needed for a provenance study? *Earth Planet. Sci. Lett.* **2004**, *224*, 441–451. [[CrossRef](#)]
37. Zhang, Y.Q.; Chen, W.; Yang, N.  $^{40}\text{Ar}/^{39}\text{Ar}$  dating of shear deformation of the Xianshuihe fault zone in west Sichuan and its tectonic significance. *Sci. China Ser. D–Earth Sci.* **2004**, *47*, 794–803.
38. Itaya, T.; Hyodo, H.; Tsujimori, T.; Wallis, S.; Aoya, M.; Kawakami, T.; Gouzu, C. Regional-scale excess Ar wave in a Barrovian type metamorphic belt, eastern Tibetan Plateau. *Island Arc* **2009**, *18*, 293–305. [[CrossRef](#)]
39. Kirby, E. *Geomorphic Insights into the Growth of Eastern Tibet and Implications for the Recurrence of Great Earthquakes*; AGU Fall Meeting Abstracts: Washington, DC, USA, 2008; p. 3.
40. Kirby, E.; Reiners, P.W.; Krol, M.A.; Whipple, K.X.; Hodges, K.V.; Farley, K.A.; Tang, W.Q.; Chen, Z.L. Late cenozoic evolution of the eastern Margin of the Tibetan Plateau: Inferences from  $^{40}\text{Ar}/^{39}\text{Ar}$  and (U–Th)/He thermochronology. *Tectonics* **2002**, *21*. [[CrossRef](#)]
41. Godard, V.; Pik, R.; Lave, J.; Cattin, R.; Tibari, B.; de Sigoyer, J.; Pubellier, M.; Zhu, J. Late cenozoic evolution of the central Longmen shan, eastern Tibet: Insight from (U–Th)/He thermochronometry. *Tectonics* **2009**, *28*. [[CrossRef](#)]

42. Cook, K.L.; Hovius, N.; Wittmann, H.; Heimsath, A.M.; Lee, Y.-H. Causes of rapid uplift and exceptional topography of Gongga shan on the eastern Margin of the Tibetan Plateau. *Earth Planet. Sci. Lett.* **2018**, *481*, 328–337. [[CrossRef](#)]
43. Henck, A.C.; Huntington, K.W.; Stone, J.O.; Montgomery, D.R.; Hallet, B. Spatial controls on erosion in the Three Rivers region, southeastern Tibet and southwestern China. *Earth Planet. Sci. Lett.* **2011**, *303*, 71–83. [[CrossRef](#)]
44. Lu, Y.J.; Kerrich, R.; Cawood, P.A.; McCuaig, T.C.; Hart, C.J.R.; Li, Z.X.; Hou, Z.Q.; Bagas, L. Zircon shrimp U–Pb geochronology of potassic felsic intrusions in western Yunnan, SW China: Constraints on the relationship of Magmatism to the Jinsha suture. *Gondwana Res.* **2012**, *22*, 737–747. [[CrossRef](#)]
45. Vezzoli, G.; Garzanti, E.; Limonta, M.; Andò, S.; Yang, S.Y. Erosion patterns in the Changjiang (Yangtze River) catchment revealed by bulk-sample versus single-mineral provenance budgets. *Geomorphology* **2016**, *261*, 177–192. [[CrossRef](#)]
46. McDougall, I.; Harrison, T.M. *Geochronology and Thermochronology by the  $^{40}\text{Ar}/^{39}\text{Ar}$  Method*; Oxford University Press on Demand: Oxford, UK, 1999.
47. Enkelmann, E.; Weislogel, A.; Ratschbacher, L.; Eide, E.; Renno, A.; Wooden, J. How was the triassic Songpan-Ganzi basin filled? A provenance study. *Tectonics* **2007**, *26*. [[CrossRef](#)]
48. Weislogel, A.L.; Graham, S.A.; Chang, E.Z.; Wooden, J.L.; Gehrels, G.E. Detrital zircon provenance from three turbidite depocenters of the middle-upper triassic Songpan-Ganzi complex, central China: Record of collisional tectonics, erosional exhumation, and sediment production. *Geol. Soc. Am. Bull.* **2010**, *122*, 2041–2062. [[CrossRef](#)]
49. Weislogel, A.L.; Graham, S.A.; Chang, E.Z.; Wooden, J.L.; Gehrels, G.E.; Yang, H.S. Detrital zircon provenance of the late triassic Songpan-Ganzi complex: Sedimentary record of collision of the north and south China blocks. *Geology* **2006**, *34*, 97–100. [[CrossRef](#)]
50. Yan, Z.K.; Tian, Y.T.; Li, R.; Vermeesch, P.; Sun, X.L.; Li, Y.; Rittner, M.; Carter, A.; Shao, C.J.; Huang, H.; et al. Late Triassic tectonic inversion in the upper Yangtze Block: Insights from detrital zircon U–Pb geochronology from south-western Sichuan basin. *Basin Res.* **2019**, *31*, 92–113. [[CrossRef](#)]
51. She, Z.B.; Ma, C.Q.; Wan, Y.S.; Zhang, J.Y.; Li, M.; Chen, L.; Xu, W.J.; Li, Y.Q.; Ye, L.F.; Gao, J. An early Mesozoic transcontinental palaeoriver in south China: Evidence from detrital zircon U–Pb geochronology and Hf isotopes. *J. Geol. Soc.* **2012**, *169*, 353–362. [[CrossRef](#)]
52. Jolivet, M.; Roger, F.; Xu, Z.Q.; Paquette, J.L.; Cao, H. Mesozoic–Cenozoic evolution of the Danba dome (Songpan Garzê, east Tibet) as inferred from LA-ICPMS U–Pb and fission-track data. *J. Asian Earth Sci.* **2015**, *102*, 180–204. [[CrossRef](#)]
53. Roberts, N.M.W.; Searle, M.P. Zircon U–Pb–Hf constraints from Gongga Shan granites on young crustal melting in eastern Tibet. *Geosci. Front.* **2019**, *10*, 885–894. [[CrossRef](#)]
54. Schwartz, T.M.; Schwartz, R.K.; Weislogel, A.L. Orogenic recycling of detrital zircons characterizes age distributions of north American cordilleran strata. *Tectonics* **2019**, *38*, 4320–4334. [[CrossRef](#)]
55. Wang, W.T.; Zheng, W.J.; Zhang, P.Z.; Li, Q.; Kirby, E.; Yuan, D.Y.; Zheng, D.W.; Liu, C.C.; Wang, Z.C.; Zhang, H.P.; et al. Expansion of the Tibetan Plateau during the Neogene. *Nat. Commun.* **2017**, *8*, 15887. [[CrossRef](#)] [[PubMed](#)]
56. Campbell, I.H.; Reiners, P.W.; Allen, C.M.; Nicolescu, S.; Upadhyay, R. He–Pb double dating of detrital zircons from the Ganges and Indus Rivers: Implication for quantifying sediment recycling and provenance studies. *Earth Planet. Sci. Lett.* **2005**, *237*, 402–432. [[CrossRef](#)]
57. Zimmermann, S.; Mark, C.; Chew, D.; Voice, P.J. Maximising data and precision from detrital zircon U–Pb analysis by LA-ICPMS: The use of core-rim ages and the single-analysis concordia age. *Sediment. Geol.* **2018**, *375*, 5–13. [[CrossRef](#)]
58. Hoang, L.V.; Wu, F.-Y.; Clift, P.D.; Wysocka, A.; Swierczewska, A. Evaluating the evolution of the Red River system based on in situ U–Pb dating and Hf isotope analysis of zircons. *Geochem. Geophys. Geosyst.* **2009**, *10*. [[CrossRef](#)]
59. Kong, P.; Zheng, Y.; Fu, B.H. Cosmogenic nuclide burial ages and provenance of late cenozoic deposits in the Sichuan Basin: Implications for early Quaternary glaciations in east Tibet. *Quat. Geochronol.* **2011**, *6*, 304–312. [[CrossRef](#)]
60. Zheng, H.B.; Clift, P.D.; Wang, P.; Tada, R.; Jia, J.T.; He, M.Y.; Jourdan, F. Pre-Miocene birth of the Yangtze River. *Proc. Natl. Acad. Sci. USA* **2013**, *110*, 7556–7561. [[CrossRef](#)]

61. Wang, P.; Zheng, H.; Liu, S.; Hoke, G. Late Cretaceous drainage reorganization of the middle Yangtze River. *Lithosphere* **2018**, *10*, 392–405. [[CrossRef](#)]
62. Wang, P.; Zheng, H.B.; Chen, L.; Chen, J.; Xu, Y.; Wei, X.; Yao, X. Exhumation of the Huangling anticline in the Three Gorges region: Cenozoic sedimentary record from the western Jiangnan basin, China. *Basin Res.* **2014**, *26*, 505–522. [[CrossRef](#)]
63. Wissink, G.K.; Hoke, G.D.; Garziona, C.N.; Liu-Zeng, J. Temporal and spatial patterns of sediment routing across the southeast Margin of the Tibetan Plateau: Insights from detrital zircon. *Tectonics* **2016**, *35*. [[CrossRef](#)]
64. Chen, Y.; Yan, M.D.; Fang, X.M.; Song, C.H.; Zhang, W.L.; Zan, J.B.; Zhang, Z.G.; Li, B.S.; Yang, Y.P.; Zhang, D.W. Detrital zircon U–Pb geochronological and sedimentological study of the Simao Basin, Yunnan: Implications for the early Cenozoic evolution of the Red River. *Earth Planet. Sci. Lett.* **2017**, *476*, 22–33. [[CrossRef](#)]
65. Kong, P.; Zheng, Y.; Caffee, M.W. Provenance and time constraints on the formation of the first bend of the Yangtze River. *Geochem. Geophys. Geosyst.* **2012**, *13*. [[CrossRef](#)]
66. Deng, B.; Chew, D.; Jiang, L.; Mark, C.; Cogné, N.; Wang, Z.J.; Liu, S.G. Heavy mineral analysis and detrital U–Pb ages of the intracontinental Paleo-Yangtze basin: Implications for a transcontinental source-to-sink system during late Cretaceous time. *GSA Bull.* **2018**, *130*, 2087–2109. [[CrossRef](#)]
67. Yang, C.Q.; Shen, C.B.; Zattin, M.; Yu, W.; Shi, S.X.; Mei, L.F. Provenances of Cenozoic sediments in the Jiangnan Basin and implications for the formation of the Three Gorges. *Int. Geol. Rev.* **2019**, *61*, 1980–1999. [[CrossRef](#)]



© 2020 by the authors. Licensee MDPI, Basel, Switzerland. This article is an open access article distributed under the terms and conditions of the Creative Commons Attribution (CC BY) license (<http://creativecommons.org/licenses/by/4.0/>).